Available online at www.sciencedirect.com
SCIENCE DIRECT
ELSEVIER
Journal of the European Ceramic Society 26 (2006) 2257–2264
ECERS
www.elsevier.com/locate/jeurceramsoc

Solvent effect on microstructure of yttria-stabilized zirconia (YSZ) particles in solvothermal synthesis

Zile Hua [a,b], Xin M. Wang [a], Ping Xiao [a,*], Jianlin Shi [b,*]

[a] *Manchester Materials Science Centre, University of Manchester, Grosvenor Street, Manchester M1 7HS, UK*
[b] *State Key Lab of High Performance Ceramics and Superfine Microstructure, Shanghai Institute of Ceramics, Chinese Academy of Sciences, 1295 DingXi Road, Shanghai 200050, PR China*

Received 16 February 2005; received in revised form 18 April 2005; accepted 23 April 2005
Available online 13 June 2005

Abstract

Using methanol or methanol/2-propanol mixtures as reaction media, yttria-stabilized zirconia (YSZ) particles were synthesized with a solvothermal route. The particles were characterized with X-ray diffractometry (XRD), scanning electron microscopy (SEM), transmission electron microscopy (TEM), laser diffraction technique, and nitrogen adsorption isotherms. Results indicated that cubic/tetragonal YSZ nanocrystals with crystal size lower than 5 nm were obtained and the crystal size depends on solvent composition, reaction temperature and reaction time. For the same reaction temperature and reaction time, the solvent composition also controls YSZ crystal agglomeration behaviour. According to the DLVO theory and analysis of experimental results, the solvent effect on microstructures of YSZ particles in solvothermal synthesis has been discussed. In addition, the mechanism of particle microstructure evolution during solvothermal synthesis has been suggested.

Keywords: ZrO_2; Powders-chemical preparation; Solvothermal synthesis

1. Introduction

Due to their high performances in mechanical, thermal, electrical, ionic conducting, optical, and catalytic properties, zirconia-based ceramics have attracted extensive interests in academia and industry for a long time.[1–3] In recent years, many studies have been focused on preparation and characterization of nanophased zirconia consisted of nanosized grains.[4–5] Compared with conventional ceramics made up of microsized grains, nanophased ceramics not only possess better and/or some novel properties, but also achieve a lower sintering/post thermal-treating temperature resulting from higher reactivity of nanosized powder precursors. The latter is a prerequisite for a wide range of applications of nanoceramics. Therefore, how to control the processing parameters to obtain soft agglomerated or even nonagglomerated nanosized powder precursors becomes a first and decisive step for the preparation of nanophased ceramics. So far a number of chemical processes, such as homogeneous precipitation,[6] spray pyrolysis,[7] sol–gel[8] and nonhydrolytic sol–gel[9], and hydrothermal synthesis[1,10] have been developed for the preparation of nanosized zirconia-based ceramics powders. Very recently, using ethanol or ethanol/2-propanol mixtures as reaction media, our group has reported the solvothermal synthesis of yttria-stabilized zirconia (YSZ) nanocrystals (about 3.5 nm) with soft agglomerates in a simple one-step processing.[11] To the best of our knowledge, the synthesized YSZ nanocrystals possess the lowest agglomerate sizes (0.12–0.18 μm) among the ever-reported zirconia-based nanopowders.

Here, to further clarify the solvent effect on microstructures of YSZ particles in solvothermal synthesis, we extended the choice of organic solvents to methanol or methanol/2-propanol mixtures. Also, as a comparison, hydrothermal

* Corresponding authors. Tel.: +44 161 200 5941; fax: +44 161 200 3586.
E-mail addresses: ping.xiao@manchester.ac.uk (P. Xiao), jlshi@sunm.shcnc.ac.cn (J. Shi).

0955-2219/$ – see front matter © 2005 Elsevier Ltd. All rights reserved.
doi:10.1016/j.jeurceramsoc.2005.04.021

synthesis of YSZ particles was also conducted under the identical condition. Results indicated that either soft YSZ agglomerates or YSZ aggregates (hard-agglomerates) had been formed, which strongly depended on the solvent composition. Based on the DLVO theory, sol–gel chemistry, and zeta potential measurements, the factors controlling particle agglomeration/aggregation, such as electrical double layers, and steric effect of surface organic groups are discussed.

2. Experimental procedure

2.1. Materials synthesis

The starting materials include zirconyl chloride octahydrate ($ZrOCl_2{\cdot}8H_2O$, 98%), yttrium chloride (YCl_3, 99.9%), and methanol (CH_3OH, 99.8%), which are from Sigma-Aldrich Co. Ethanol (CH_3CH_2OH, >99.86%) and 2-propanol ($(CH_3)_2CHOH$, Laboratory Reagent Grade) were purchased from Fisher Scientific UK Limited and HAYMAN Limited, respectively. All chemicals were used without further purification. According to the stoichiometric composition of $(ZrO_2)_{0.95}(Y_2O_3)_{0.05}$ with 0.05 mol L^{-1} zirconium ions concentration, $ZrOCl_2{\cdot}8H_2O$ and YCl_3 were dissolved in methanol or methanol/2-propanol mixtures with volume ratios ($v_{MeoH}/v_{2\text{-}PrOH}$) of 40/60, 20/80, and 10/90. After continuous stirring for 12–24 h, a homogeneous and clear solution was obtained, which indicated a complete dissolution of metal salt precursors. The resulting solution was poured into a polytetrafluoroethylene (PTFE) tube and then placed into a stainless-steel autoclave with a surrounding external heater (Autoclaves Engineers Co., USA). Solvothermal synthesis was performed at 160–200 °C for 2–72 h under the autogenous pressure. After the autoclave being cooled down to room temperature, the product was collected by centrifugation and washed with ethanol repeatedly until no Cl^- ions were detected in the supernatant with $AgNO_3$ solution (0.1 mol L^{-1}). The product was then dried in a vacuum desiccator.

2.2. Characterization

X-ray diffractometry (XRD) analysis of the YSZ powder was made using a Philips PW 1120/90 diffractometer with Cu Kα radiation at 50 kV and 40 mA. The samples were scanned from 20° to 80° 2θ with a scanning rate of 0.008°/s and a step size of 0.05°. The average crystal size D was calculated using Scherrer's Eq. (1):

$$D = \frac{\kappa\lambda}{\beta\cos\theta} \tag{1}$$

where κ, λ, β, and θ are the Scherrer constant ($\kappa = 0.9$), the wavelength of Cu Kα radiation ($\lambda = 1.54056$ Å), the full width at half maximum (FWHM) of the (2 2 0) reflection of cubic/tetragonal YSZ phase, and the Bragg angle of the (2 2 0) reflection of cubic/tetragonal YSZ phase, respectively. The XRD patterns were deconvolved with pre-installed PC-APD software (Version 3.6j) to determine the peak positions and the corresponding FWHMs. Single crystal silicon was used as an external standard to calibrate instrument broadening. The agglomerate size distribution of synthesized particles was measured with a Malvern Mastersizer Mciroplus particle size analyzer. Nitrogen adsorption isotherms at 77 K were measured on a Coulter SA 3100 adsorption analyzer. All samples were outgassed at 100 °C for 2 h under vacuum before the measurement. The specific surface areas of synthesized YSZ nanocrystals were calculated based on the Brunauer–Emmet–Teller (BET) method and the average crystal sizes D_{BET} were calculated with the following Eq. (2):

$$D_{BET} = \frac{6000}{S_{BET} \times \rho} \tag{2}$$

where S_{BET} and ρ represent the specific surface areas (m^2/g) and the theoretical density (g/cm^3) of synthesized nanocrystals, respectively. Thermogravimetry and differential scanning calorimetry (TG-DSC) were carried out on a NETZSCH STA 449C with a heating rate of 5 °C/min from room temperature to 1000 °C. In addition, the crystal sizes and the agglomerate morphology of synthesized particles were also examined with Philips CM200 transmission electron microscope (TEM) operated at 200 kV and with JEOL JSM6700F field emission scanning electron microscope (FE-SEM). TEM samples were prepared by depositing the YSZ particle suspension in ethanol on a carbon-coated copper mesh grid, and then drying in air at room temperature. For SEM, the particle suspensions were dropped on a stub. After drying, the particles were coated with a carbon layer. The chemical compositions of all samples were analyzed by the energy dispersive X-ray microanalysis (EDX) instrument attached to Philips CM200 TEM. For the zeta potential measurement, the as-synthesized particles were diluted in the corresponding solvent used for synthesis and were measured using a Zeta Potential Analyzer (Brookhaven Instrument Corp.) at room temperature.

3. Results

Fig. 1 shows XRD patterns of YSZ nanocrystals synthesized in methanol at 180 °C with different reaction durations. Although there is no peak to show the presence of monoclinic phase, it is difficult to distinguish between tetragonal and cubic phases from the XRD patterns due to peak broadening resulted from the nanocrystal size effect. Therefore, all of the diffraction peaks are indexed according to the cubic symmetry. Obviously, the diffraction peaks become more intense with increase in solvothermal synthesis time, which implies the increase of crystal sizes. According to Scherrer's Eq. (1), the calculated apparent crystal sizes increase from 1.1 nm (sample (1a), 12 h) to 2.1 nm (sample (1b), 24 h) and then to 3.4 nm (sample (1c), 48 h). This phenomenon is different from our previous results about solvothermal synthesis of

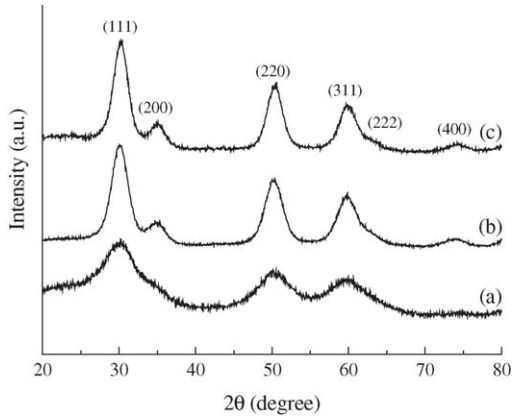

Fig. 1. XRD patterns of nanosized YSZ particles synthesized in different time durations for 0.05 M $ZrOCl_2{\cdot}8H_2O$ in methanol at 180 °C (a) 12 h (crystal size: 1.1 nm), (b) 24 h (2.1 nm) and (c) 48 h (3.4 nm).

YSZ nanocrystals with ethanol or ethanol/2-propanol mixtures as reaction media, which shows no obvious crystal growth up to 48 h (about 3.5 nm). In addition, the agglomerate sizes of this synthesized YSZ particles, shown in Fig. 2 are not as small as those obtained in ethanol or ethanol/2-propanol mixtures (0.12–0.18 μm)[11], although it decreases to 2.53 μm with synthesis time extending to 48 h (Fig. 2 (c)).

Being consistent with above particle-size measurement and XRD analysis results, Figs. 3 and 4 show TEM and SEM images of sample 1(b) synthesized in methanol at 180 °C for 24 h. The images indicate that when methanol was used as the reaction media, the obtained particles are spherical aggregates and among them, part of smaller-sized aggregates fuses together to form the irregularly-shaped ones, which is different from the soft agglomerates of YSZ nanocrystals synthesized in ethanol or ethanol/2-propanol mixtures.[11] This difference in YSZ particles morphology due to use of different solvents will be further examined later and discussed in light of the sol–gel chemistry knowledge and DLVO theory of the colloidal stability. In Fig. 3, the inset SAED (selected

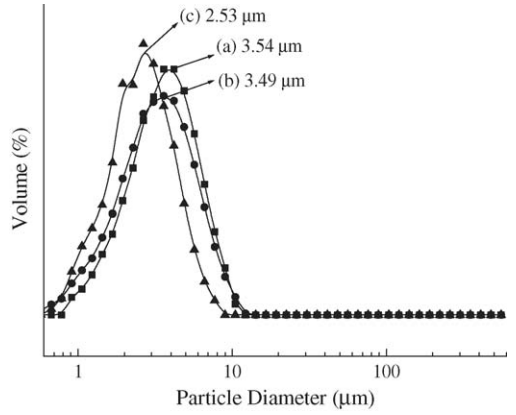

Fig. 2. Agglomerate size distribution of nanosized YSZ particles synthesized in different time durations for 0.05 M $ZrOCl_2{\cdot}8H_2O$ in methanol at 180 °C (a) 12 h, (b) 24 h and (c) 48 h.

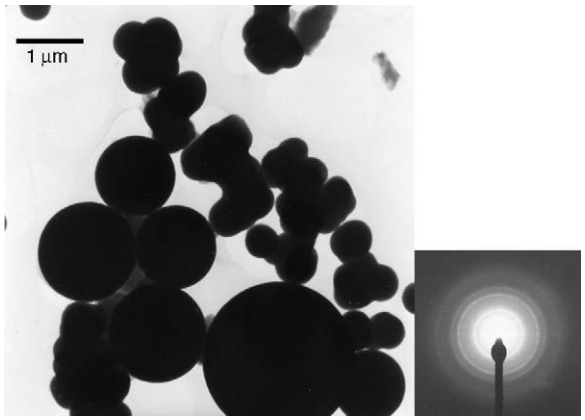

Fig. 3. TEM image and SAED pattern of YSZ particles synthesized in methanol at 180 °C for 24 h.

area electron diffraction) pattern could be indexed as the face-centered cubic phase.

Fig. 5 shows XRD patterns of YSZ nanocrystals synthesized at 200 °C for 2 h in methanol/2-propanol mixtures with different volume ratios. It could be found that decreasing the volume content of methanol in the reaction media accelerates

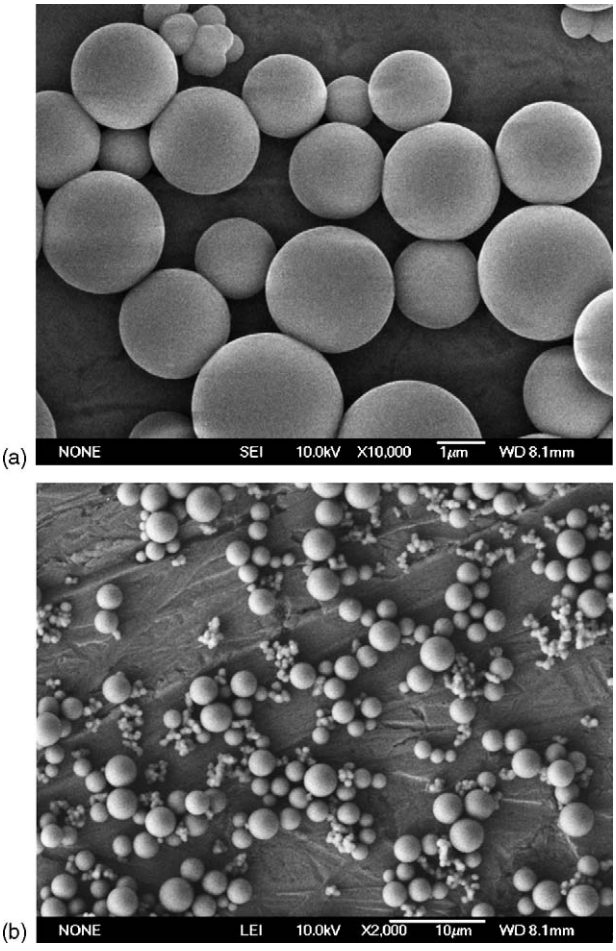

Fig. 4. SEM images of YSZ particles synthesized in methanol at 180 °C for 24 h.

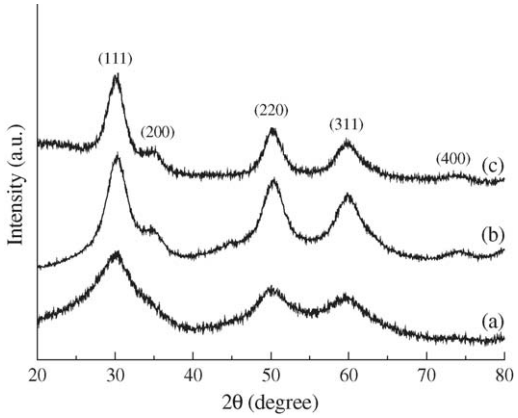

Fig. 5. XRD patterns of YSZ nanocrystals synthesized for 0.05 M $ZrOCl_2{\cdot}8H_2O$ at 200 °C for 2 h in methanol–2-propanol mixtures solvent with different volume ratios ($v_{MeoH}/v_{2\text{-}PrOH}$) (a) 40/60 (crystal size: 1.3 nm), (b) 20/80 (1.9 nm) and (c) 10/90 (2.7 nm).

the crystal growth and eventually increases the crystal sizes of YSZ products. According to Scherrer's Eq. (1), the calculated apparent crystal sizes increase from 1.3 nm of sample (5a) to 1.9 nm of (5b) and then to 2.7 nm of (5c) with increase in the methanol/2-propanol ratio. Moreover, the agglomerate size, as shown in Fig. 6, decreases with decrease in the methanol/2-propanol ratio with reaction time as 2 h. When $v_{MeoH}/v_{2\text{-}PrOH}$ reaches 10/90, a product with agglomerate size of 0.77 μm is obtained. It implies the different microstructures of the synthesized products were obtained when the solvent compositions was changed. Further, when the reaction time increases to 12, 24, or 72 h, YSZ nanocrystal growth has also been observed (as shown in Fig. 7, the apparent crystallite sizes increase from 2.7 nm of sample (7a, 2 h) to 3.5 nm of (7b, 12 h) to 3.9 nm of (7c, 24 h) and then to 4.1 nm of (7d, 72 h)). But the increase is not significant as that shown in Fig. 1 for samples synthesized in methanol. Actually, after 12 h reaction, the crystal growth rate has become very slow. When the reaction time is longer than 24 h, the crystal growth is almost

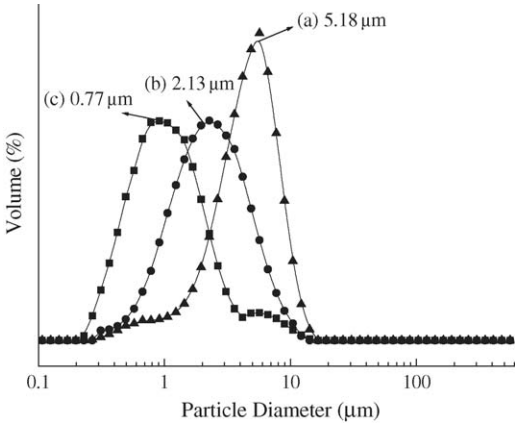

Fig. 6. Agglomerate size distribution of nanosized YSZ particles synthesized for 0.05 M $ZrOCl_2{\cdot}8H_2O$ at 200 °C with reaction time of 2 h in methanol-2-propanol mixed solvent with different volume ratios ($v_{MeoH}/v_{2\text{-}PrOH}$) (a) 40/60, (b) 20/80 and (c) 10/90.

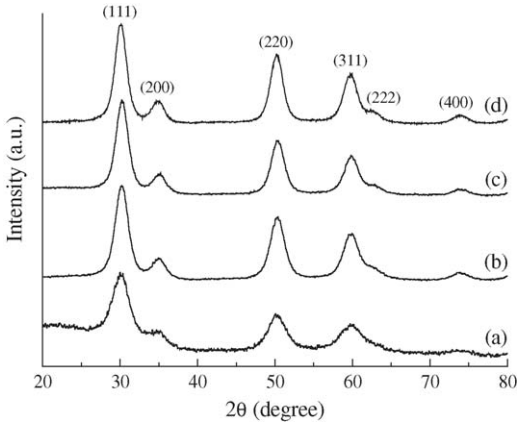

Fig. 7. XRD patterns of nanosized YSZ particles synthesized for 0.05 M $ZrOCl_2{\cdot}8H_2O$ at 200 °C in 10/90 ($v_{MeoH}/v_{2\text{-}PrOH}$) methanol–2-propanol mixed solvent in different time durations (a) 2 h (crystal size: 2.7 nm), (b) 12 h (3.5 nm), (c) 24 h (3.9 nm) and (d) 72 h (4.1 nm).

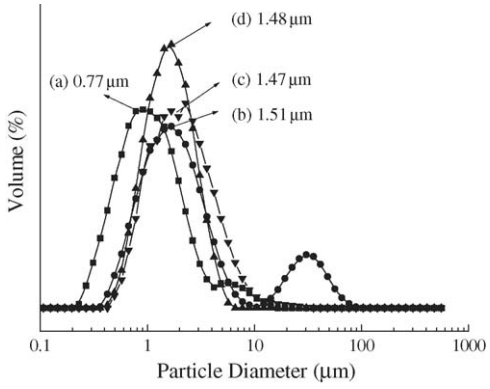

Fig. 8. Agglomerate size distribution of nanosized YSZ particles synthesized for 0.05 M ZrOCl2·8H2O at 200 °C in 10/90 ($v_{MeoH}/v_{2\text{-}PrOH}$) methanol–2-propanol mixed solvent in different time durations (a) 2 h, (b) 12 h, (c) 24 h and (d) 72 h.

negligible. Simultaneously, the agglomerate size also reaches constant, i.e. 1.50 μm (Fig. 8). A similar phenomenon was shown in our previous report about YSZ nanocrystals synthesis in ethanol or ethanol/2-propanol, although crystal growth almost stopped after a shorter reaction period (less than 2 h). Table 1 summarizes crystal sizes and BET specific surface areas of YSZ nanocrystals synthesized in the 10/90 (v/v) methanol/2-propanol mixture at 200 °C for different reaction

Table 1
Characteristics of YSZ nanocrystals solvothermally synthesized in 10/90 (v/v) methanol/2-propanol at 200 °C for different time durations

Sample	Reaction time (h)	S_{BET} (m_2/g)	D_{BET} (nm)	D (nm)	D^* (nm)
7(a)	2	247	4.0	2.7	2.5
7(b)	12	227	4.4	3.5	3.5
7(c)	24	214	4.7	3.9	–
7(d)	72	187	5.3	4.1	4.0

D_{BET}: calculated with Eq. (2) and ρ of 6.02 g/cm^3. D: calculated with Scherrer's Eq. (1). D^*: crystal size after nitrogen adsorption isotherms measurement calculated with Scherrer's Eq. (1).

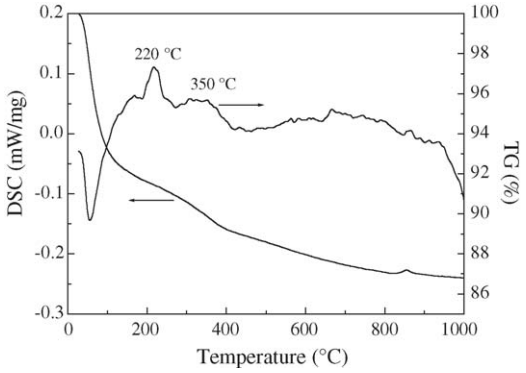

Fig. 9. TG-DSC curves of YSZ nanocrystals synthesized in 10/90 (v/v) methanol/2-propanol mixture at 200 °C for 24 h.

time. A slight discrepancy between D_{BET} and D is found. Although the consistence between D and D^* excludes the possibility of crystal growth during thermal treatment before nitrogen adsorption isotherms measurement, the increase of inter-bridging effect among YSZ nanocrystals or even some aggregation resulted from this thermal treatment should be inevitable. According to Eq. (2), it leads to the decrease of S_{BET} and consequently the increase of D_{BET}.

Fig. 9 shows TG-DSC curves of YSZ nanocrystals synthesized in 10/90 (v/v) methanol/2-propanol mixture at 200 °C for 24 h. Major weight loss (8 wt.%) appears from room temperature to 100 °C and the endothermal peak corresponds to the desorption of physically absorbed organic solvents and water. Both broad exothermal peaks around 220 and 350 °C correspond to the elimination of powder surface-bound water and organics formed during solvothermal synthesis or subsequent ethanol-washing process.[12,13] The resulted weight loss is about 3 wt.%. No additional exothermal peak appears in the range of 400–500 °C, which is due to the crystallization of amorphous zirconia,[13,14] which excludes the possibility of formation of amorphous phase in the solvothermal synthesis.

Fig. 10 is TEM images and the corresponding SAED pattern of YSZ nanocrystals synthesized in 40/60 (v/v) methanol/2-propanol mixture at 200 °C for 2 h and in 10/90 (v/v) methanol/2-propanol mixture at 200 °C for 24 h, respectively. The former (Fig. 10(a)) is similar with YSZ particles synthesized in methanol solvent (Fig. 3) where both isolated spherical aggregates or irregularly-shaped ones can be observed. It implies that in this synthesis situation, particle agglomeration behavior is close to that happened when methanol was used as the reaction media. On the other hand, in Fig. 10(b), when 10/90 (v/v) methanol/2-propanol mixed solvent was used, highly dispersed nanocrystals and clear crystal lattices could be found, which is similar to the microstructure of YSZ nanocrystals obtained in ethanol or ethanol/2-propanol mixtures solvent.[11] EDX analysis corresponding to Fig. 10(b) reveals the elemental composition ratio of Zr:Y ≅ 15:1. The yttrium content is lower than that of the starting composition of $(ZrO_2)_{0.95}(Y_2O_3)_{0.05}$ (Zr:Y ≅ 9.5:1)

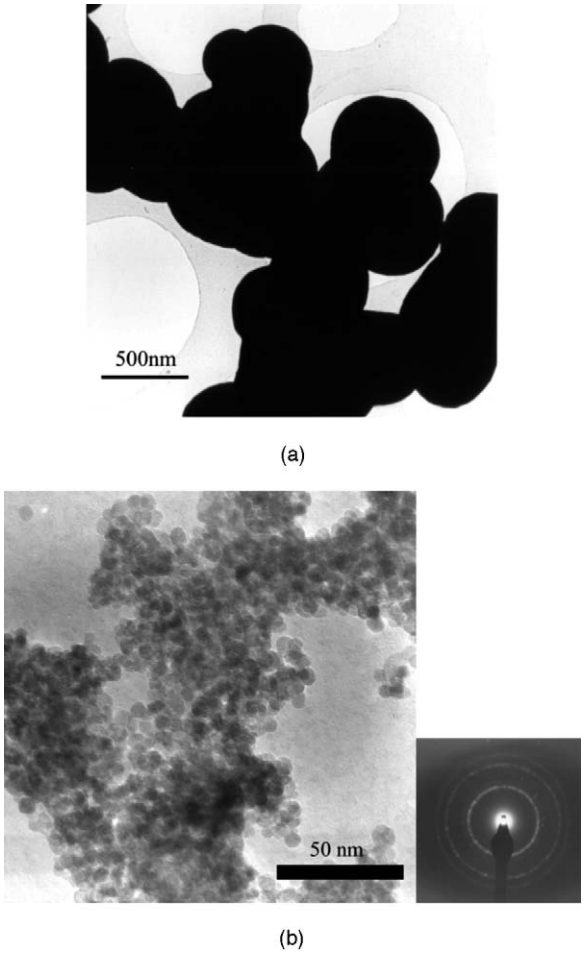

Fig. 10. TEM images and SAED pattern of YSZ particles synthesized at 200 °C in methanol/2-propanol mixture (a) 40/60 (v/v) for 2 h and (b) 10/90 (v/v) for 24 h.

because under the acidic solvothermal condition, part of yttrium has been dissolved in the reaction media.

4. Discussion

Use of $ZrOCl_2{\cdot}8H_2O$ for preparation of nanophased zirconia-based ceramics is a common practice now. In most cases, water is used as the reaction medium. Because $ZrOCl_2{\cdot}8H_2O$ crystal does not truly contain zirconyl ions, i.e. ZrO^{2+}, but the tetrameric ions $[Zr(OH)_2{\cdot}4H_2O]_4{}^{8+}$, it is argued that when $ZrOCl_2{\cdot}8H_2O$ is dissolved into an aqueous solution with $[Zr(OH)_2{\cdot}4H_2O]_4{}^{8+}$ ions present as the major species.[2] The four zirconium atoms in each unit are arranged in a square, and each zirconium atom is coordinated by four bridging OH groups and four H_2O molecules. Due to the deprotonation effect as shown in Eq. (3), the tetrameric ions release H^+ ions from the coordinated water and consequently add some nonbridging hydroxyl groups on the zirconium atoms. Then the polymerization reaction happens (Eq. (4)) among these newly formed tetrameric ions

$[Zr(OH)_{2+x}\cdot(4-x)H_2O]_4^{(8-4x)+}$ to form polymeric species and ultimately the nucleus of hydrous zirconia.

$$[Zr(OH)_2\cdot 4H_2O]_4^{8+} \leftrightarrow [Zr(OH)_{2+x}\cdot(4-x)H_2O]_4^{(8-4x)+} + 4xH^+ \quad (3)$$

$$\leftrightarrow [ZrO_y(OH)_{2+x-2y}\cdot zH_2O]_n + mH_2O \quad (4)$$

However, at room temperature, the above-mentioned reaction (3) and (4) are very slow and $ZrOCl_2\cdot 8H_2O$ aqueous solution is usually stable both thermodynamically and kinetically.[15] It does not lead to nucleation and crystal-growth. Heating or/and addition of base causes the equilibrium of Eq. (3) to shift toward the right and the concentration of $[Zr(OH)_{2+x}\cdot(4-x)H_2O]_4^{(8-4x)+}$ ions and $[ZrO_y(OH)_{2+x-2y}\cdot zH_2O]_n$ increase. When their concentrations reach a critical supersaturation level, nucleus of hydrous zirconia are generated and followed by the crystal-growth to form primary particles and then agglomerations among primary particles.

However, when organic solvents, i.e. alkyl alcohols, are adopted as the reaction media as in our experiments, some changes should be considered. First, alkoxyl groups would partially substitute the nonbridging hydroxyl group, as reported in previous reports.[13] Under the circumstances, the tetrameric ions should be $[Zr(OM)_{2+x}\cdot(4-x)H_2O]_4^{(8-4x)+}$ (M = methyl, ethyl, isopropyl, etc.) rather than $[Zr(OH)_{2+x}\cdot(4-x)H_2O]_4^{(8-4x)+}$. As a result, it would affect the subsequent polymerization kinetics, not only because of the steric effect of organic ligands, but also the change of partial charge.[12,13,16] Therefore, the reaction rate and the reaction equilibrium point would depend on the properties of the alkoxyl groups and also of the solvents. Second, from the description above, it should be known that only after a critical supersaturation level were reached, the nucleation and crystal-growth processes for the formation of primary particles would take place. Consequently, the supersaturation degree, which would be different in different solvents, would influence the nucleation numbers, the crystal-growth rates and the product yields in this process.

Now we can analyses the results shown in Figs. 1, 5 and 7. Because each solvent possesses its specific dielectric constant, which corresponds to the specific solubility of the inorganic solute and consequently the specific supersaturation degree in the reaction system, under the other identical reaction conditions, when methanol, ethanol, 2-propanol or mixed solvent is used as the reaction media respectively, it shows different crystallization behaviors. In methanol solvent, a higher dielectric constant ($\varepsilon = 32.6$) corresponds to a higher solubility of the inorganic solute and a lower supersaturation degree in this system, which predicts less nucleation numbers and slower crystal-growth rates. Therefore, as shown in Fig. 1, after a 12 h reaction, YSZ nanocrystals with smaller size (1.1 nm) is obtained and with increase in reaction time, crystals grow slowly. Even after the 24 h reaction, YSZ nanocrystals of 2.1 nm could be only obtained. On the other hand, in a mixed solvent of 10/90 (v/v) methanol/2-propanol ($\varepsilon = 20.9$) (Fig. 7), just after a 2 h reaction, YSZ nanocrystals of 2.7 nm is already produced and after the 24 h reaction, nanocrystals with a relatively stable size of 3.9 nm is obtained and then the crystal growth almost stops even with increase in the reaction time to 72 h.

In this experiment, another interesting result is that the particles agglomerate states depend on the solvent compositions. When methanol is used as the major solvent, spherical aggregates are formed, which are made up of nanocrystals, not amorphous materials as reported by others.[17] Considering the energy barrier for particles agglomeration and steric effect of surface organic groups, DLVO theory could be used to explain the phenomenon.

According to DLVO theory,[18] when considering the identical spherical particles in the colloidal system, the energy barrier (V) for agglomeration between two particles could be expressed as Eqs. (5)–(8)

$$V = V_A + V_R \quad (5)$$

$$V_A = -\frac{Aa}{12H_0} \quad (6)$$

$$V_R = \frac{\varepsilon_0\varepsilon_r a\psi_0^2}{2}\ln[1+\exp(-\kappa H_0)] \quad (7)$$

$$\kappa = \left(\frac{8\pi c e^2 z^2}{\varepsilon_0\varepsilon_r\kappa_B T}\right)^{1/2} \quad (8)$$

where V_A is the potential energy of Van der Waals-London attractive force, V_R the potential energy of electrical double layer repulsion force, A the Hamaker constant, a the particle radii, H_0 the shortest distance between the surfaces of the two particles, κ the Debye-Hückel reciprocal length parameter, ε_0 and ε_r the dielectric constant of vacuum and the reaction medium, ψ_0 the surface potential, c the number concentration of the ionic species, z the valence of the same ionic species, e the electronic charge, κ_B the Boltzmann constant, and T the absolute temperature. It has been recognized that the Hamaker constant depends on the solvent composition.[19] In our experiment, since water and alkyl alcohols possess the similar Hamaker constant,[17,20] e.g. $\sim 10^{-20}$ J for both water and ethanol, so the difference in the Hamaker constants would not significantly influence the V_A value. On the other hand, under the similar reaction conditions, the resulting parameters a and H_0 should not change significantly for the reaction systems studied here. Therefore, the V_A in Eq. (5) could be approximately constant and the whole energy barrier V would be mainly determined by the V_R item. Consequently, ε_r and ψ_0 become the determining parameters on the energy barrier V. Higher dielectric constant and larger surface potential would lead to the increase of the energy barrier V, which would be in favor of preventing particles agglomeration.

Table 2 lists the solvent dielectric constants, the zeta potentials, and the particle agglomerate morphology synthesized in different reaction media. Among them, a hydrothermal synthesis was carried out as a comparison experiment. It is

Table 2
Dielectric constants of different solvents, zeta potentials and microstructures of synthesized YSZ particles in each solvent

Solvent	Dielectric constant[a]	Zeta potential (mV)	Microstructure
Water[b]	80.1	56.6	Irregular aggregates
Methanol	32.6	58.9	Spherical aggregates
Methanol/2-propanol, 40/60 (v/v)	26.3	54.4	Spherical aggregates
Methanol/2-propanol, 10/90 (v/v)	20.9	22.5	Soft agglomerates
Ethanol/2-propanol, 60/40 (v/v)[11]	21	28.3	Soft agglomerates

[a] Dielectric constants of mixed solvents were calculated with equation $\varepsilon = \phi_1\varepsilon_1 + \phi_2\varepsilon_2$ (ϕ_i is molar percentage of each solvent).
[b] Hydrothermal product was the mixture of monoclinic and tetragonal zirconia, not YSZ, because of the high solubility of yttrium in acidic aqueous solution. In addition, the mother liquid was diluted with deionized water to carry out the zeta potentials test.

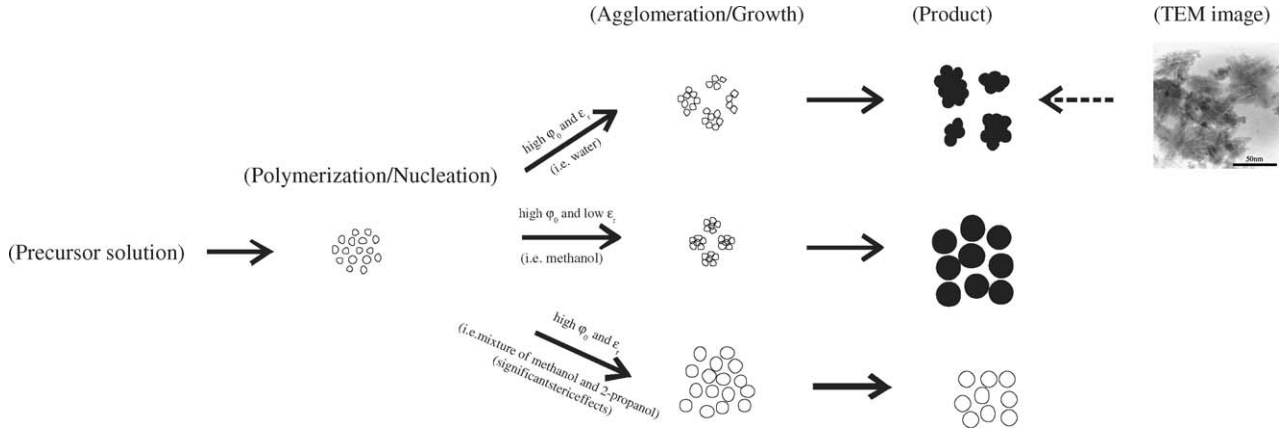

Fig. 11. Schematics of solvent effect on structure evolution of YSZ particles in solvothermal synthesis.

well-known that for the hydrous products, the "bridging" hydrogen bonds between surface hydroxyl group would evolve into the actual chemical bonds in the following drying process and lead to the formation of hard aggregates.[12] Therefore, it can be found that in this case, higher dielectric constant of water and larger surface potential of particles did not lead to formation of zirconia nanocrystals soft agglomerate due to the high energy barrier, but formation of irregularly shaped aggregates, as shown in Table 2 and Fig. 11. Therefore, the particle surface chemistry determined the particle aggregation behaviour. When methanol or 40/60 (v/v) methanol/2-propanol were used as reaction media, decrease in dielectric constant resulted in decrease in the energy barrier (V) for particles agglomeration. In this case, spherical aggregates are formed, as shown in Figs. 3 and 4. When 10/90 (v/v) methanol/2-propanol or 60/40 (v/v) ethanol/2-propanol mixture were used as reaction media, they have the lowest dielectric constants and the lowest surface potentials among the listed reaction systems, however, the products are the soft agglomerates, as shown in Fig. 10(b). Therefore, the larger volume and higher chemical stability of ethoxyl or 2-propoxyl groups compared with those of methoxyl and hydroxyl groups are the major reasons for the agglomeration behaviour.[12,13,16] Under this circumstance, the steric effect of surface organic groups should be more dominant, which favors the stability of nanocrystals and the formation of soft agglomerates. According to the above results and discussion, Fig. 11 summarizes the particles microstructure evolution during solvothermal synthesis in different solvents.

5. Conclusions

In this study, agglomerates or aggregates of tetragonal/cubic YSZ nanocrystals had been prepared with a solvothermal method. Experimental results indicated that the obtained YSZ particles agglomerate states strongly depended on the solvent compositions. Based on the DLVO theory, sol–gel chemistry, and zeta potential values, the factors, such as electrical double layer and steric effect of surface organic groups, have been confirmed to influence the particles agglomerate states in the synthesis. When methanol was used as the major part of the reaction media, the decrease of the energy barrier V resulting from lower dielectric constant of solvent would favor the formation of the spherical aggregates (hard-agglomerates). However, when more bulky organic solvents were used (e.g. ethanol or 2-propanol as the major part of the reaction media) and consequently the steric effect of the surface organic groups became more significant, soft agglomerated YSZ nanocrystals were formed. Based on these results, particles structure evolution in solvothermal synthesis has also been presented in different solvents. In addition, a direct and one-step method for the preparation of crystallized YSZ spherical aggregates is also reported here

for the first time. Further experiment is being carried out for the control of the size and distribution of the aggregates.

Acknowledgements

This work was supported by a Royal Society Research Grant and the Natural Science Foundation of China (grant no. 50232050).

References

1. Burkin, A. R., Saricimen, H. and Steele, B. C. H., Preparation of yttria stabilized zriconia (YSZ) powders by high temperature hydrolysis (HTH). *Trans. J. Br. Ceram. Soc.*, 1980, **79**, 105–108.
2. Clearfield, A., Serrette, G. P. D. and Khazi-Syed, A. H., Nature of hydrous zirconia and sulfated hydrous zirconia. *Catal. Today*, 1994, **20**, 295–312.
3. Tompsett, G. A., Sammes, N. M. and Yamamoto, O., Ceria-yttria-stabilized zirconia composite ceramic systems for applications as low-temperature electrolytes. *J. Am. Ceram. Soc.*, 1997, **80**(12), 3181–3186.
4. Shi, J. L., Gao, J. H., Lin, Z. X. and Yen, T. S., Sintering behavior of fully agglomerated zirconia compacts. *Am. Ceram. Soc.*, 1991, **74**(5), 994–997.
5. Vasylkiv, O. and Sakka, Y., Hydroxide synthesis, colloidal processing and sintering of nano-sized 3Y-TZP powder. *Scripta Mater.*, 2001, **44**(8–9), 2219–2223.
6. Vasylkiv, O. and Sakka, Y., Synthesis and colloidal processing of zirconia nanopowder. *J. Am. Ceram. Soc.*, 2001, **84**(11), 2489–2494.
7. Djurado, E. and Meunier, E., Synthesis of doped and undoped nanopowders of tetragonal polycrystalline zirconia (TPZ) by spray-pyrolysis. *J. Solid State Chem.*, 1998, **141**, 191–198.
8. Hu, M. Z.-C., Andrew Payzant, E. and Byers, C. H., Sol–gel and ultrafine particle formation via dielectric tuning of inorganic salt–alcohol–water solutions. *J. Colloid Interface Sci.*, 2000, **222**, 20–36.
9. Joo, J., Yu, T., Kim, Y. W., Park, H. M., Wu, F., Zhang, J. Z. *et al.*, Multigram scale synthesis and characterization of monodisperse tetragonal zirconia nanocrystals. *J. Am. Chem. Soc.*, 2003, **125**, 6553–6557.
10. S¯omiya, S. and Akiba, T., Hydrothermal zirconia powders: a bibliography. *J. Eur. Ceram. Soc.*, 1999, **19**, 81–87.
11. Wang, X. M., Lorimer, G. and Xiao, P., Solvothermal synthesis and processing of yttria-stabilized zirconia nanopowder. *J. Am. Ceram. Soc.*, 2005, **88**(4), 809–816.
12. Kaliszewski, M. S. and Heuer, A. H., Alcohol interaction with zirconia powders. *J. Am. Ceram. Soc.*, 1990, **73**(6), 1504–1509.
13. Caracoche, M. C., Rivas, P. C., Cervera, M. M., Caruso, Ricardo, Benavídez, E., de Sanctis, O. *et al.*, Zirconium oxide structure prepared by the sol–gel route: I. The role of the alcoholic solvent. *J. Am. Ceram. Soc.*, 2000, **83**(2), 377–384.
14. Picquart, M., López, T., Gómez, R., Torres, E., Moreno, A. and Garcia, J., Dehydration and crystallization process in sol–gel zirconia: thermal and spectroscopic study. *J. Therm. Anal. Calorim.*, 2004, **76**, 755–761.
15. Hu, M. Z.-C., Payzant, A. E. and Byers, C. H., Sol–gel and ultrafine particle formation via dielectric tuning of inorganic salt–alcohol–water solutions. *J. Colloid Interface Sci.*, 2000, **222**, 20–36.
16. Brinker, C. J. and Scherer, G. W., *Sol–Gel Science: The Physics and Chemistry of Sol–Gel Processing*. Academic Press, San Diego, 1990.
17. Moon, Y. T., Park, H. K., Kim, D. K. and Kim, C. H., Preparation of monodisperse and spherical zirconia powders by heating of alcohol-aqueous salt solutions. *J. Am. Ceram. Soc.*, 1995, **78**(10), 2690–2694.
18. Hogg, R., Healy, T. W. and Fuerstenau, D. W., Mutual coagulation of colloidal dispersions. *Trans. Faraday Soc.*, 1966, **62**, 1638–1651.
19. Hunter, R. J., *Foundations of Colloid Science*. Clarendon Press, Oxford, UK, 1987.
20. Park, H. K., Kim, D. K. and Kim, C. H., Effect of solvent on titania particle formation and morphology in thermal hydrolysis of $TiCl_4$. *J. Am. Ceram. Soc.*, 1997, **80**(3), 743–749.